VI CONGRESSO NACIONAL DE ENGENHARIA MECÂNICA
VI NATIONAL CONGRESS OF MECHANICAL ENGINEERING
18 a 21 de agosto de 2010 – Campina Grande – Paraíba - Brasil
August 18 – 21, 2010 – Campina Grande – Paraíba – Brazil

NUMERICAL ANALYSIS OF MIXED CONVECTION FLOW IN SQUARE ENCLOSURE PARTIALLY HEATED FROM BELOW USING THE MULTIGRID METHOD

Maximilian Serguei Mesquita, maximilianmesquita@ceunes.ufes.br [1]
Luar Santana de Paula, luarpaula@ceunes.ufes.br [1]
Marcelo José Santos de Lemos, delemos@ita.br [2]

[1] Departamento de Engenharias e Computação – DECOM
Universidade Federal do Espírito Santo – UFES/CEUNES
29.933-415 São Mateus, ES, Brasil

[2] Departamento de Energia – IEME
Instituto Tecnológico de Aeronáutica – ITA
12.228-900 São José dos Campos, SP, Brasil

Abstract*. The present work investigates the efficiency of the Multigrid method when applied to solve two-dimensional laminar steady mixed convection flow in a square enclosure with an partially heated from below is investigated numerically. Simulations are performed for two kinds of length of the heated source, i.e, small and large source corresponding to 10% , 30% , 50% and 100% of total length of the bottom wall, respectively. The numerical method includes finite volume discretization with upwind scheme on structure orthogonal regular meshes. Performance of the correction storage (CS) Multigrid algorithm is compared for different numbers of sweeps in each grid level. Up to four grids, for both Multigrid V- and W- cycles ,streamlines and isotherms plots are presented.*

Keywords*: Multigrid, Numerical Method, Mixed Convection, Heat transfer*

1. INTRODUCTION

Generally speaking, convergence rates of single-grid numerical solutions are greatest in the beginning of calculations, slowing sensibly as the iterative process goes on. This effect becomes more significant as the mesh becomes refined. The use of large grid sizes, nevertheless, when capturing thin boundary layer properties, resolving small recirculating regions or detecting high heat transfer spots.

The reason for that hard-to-converge behavior is that iterative methods can efficiently smooth out only those Fourier error components of wavelengths smaller than or comparable to the grid size. In contrast, the Multigrid method aims to cover a broader range of wavelengths trough relaxation on more than one grid.

The number of iterations and convergence criterion in each step along consecutive grid levels visited by the algorithm determines the so-called V- and W- cycles. Within each cycle, the intermediate solution is relaxed before (pre-) and after (post-smoothing) the transportation of values to coarser (restriction) or to finer (prolongation) grids [Brandt (1977), Hackbusch (1985) and Stüben and Trottenberg (1982)].

Accordingly, Multigrid methods have been used in an ever greater number of calculations presented in the literature and can be roughly classified into two major categories. In the CS formulation, algebraic equations are solver for the corrections of the variables whereas, in the full approximation storage (FAS) scheme, the variables themselves are handled in all grid levels. It has been pointed out in the literature that the application of the CS formulation is recommended for the solution of linear problems being the FAS formulation more suitable to non-linear cases [Brandt (1977), Hackbusch (1985) and Stüben and Trottenberg (1982)]. An exception to this rule seems to be the work of [Jiang and Tucker (1991)], who reported predictions for the Navier-Stokes equations successfully applying the Multigrid CS formulation. In the literature, however, not too many attempts in solving non-linear problems with Multigrid linear operators are found.

Acknowledging the advantages of using multiple grids, [Rabi and De Lemos (2001)] presented numerical computations applying this technique to recirculating flows in several geometries of engineering interest. There, the correction storage (CS) formulation was applied to non-linear problems. Later [Rabi and De Lemos (2003)], analyzed the effect of Peclet number and the use of different solution cycles when solving the temperature field within flows with a given velocity distribution. In all those cases, the advantages in using more than one grid in iterative solution was confirmed,

furthermore, [De Lemos and Mesquita (1999)], introduced the solution of the energy equation in their Multigrid algorithm. Temperature distribution was calculated solving the whole equation set together with the flow field as well as uncoupling the momentum and energy equations. A study on optimal relaxation parameters was there reported. More recently [Mesquita and De Lemos (2000a)] analyzed the influence of the increase of points of the mesh and optimal values of the parameters of the Multigrid cycle for different geometries. Additionally, [Mesquita and De Lemos (2000a) ,Mesquita and De Lemos (2004), Mesquita and De Lemos (2005) and Mesquita and De Lemos (2007)] , presented a study on optimal convergence characteristics in solution of conductive-convective problems.

In another hand, the physical nature of buoyancy-induced flows or nature convection, and heat transfer in enclosures has been studied extensively and is reasonably well-undershooting. In addition, the enclosure geometries has been studied in heat and mass transfer (simultaneous or not) devise of its fundamental importance, and its several technologies applications, such as cooling of electronic devices, petroleum reservoir, pollutant dispersions in atmospheric, spreading chemical and nuclear waste in soil [Braga (2003)]. The free convection conditions can be imposed inside a square cavity. Heat and pollutant induce the so-called “urban heat island effect”. The causes and characteristics of this phenomenon have been discussed by many authors in the literature and consists an applications of this subject. The interactions between the buoyancy forces and a heat elements inside the cavity and the numerical analysis of Multigrid solution applies a momentum and heat transfer forms the mains objective of current work.

2. GOVERNING EQUATIONS

The mathematical description of fluid flow and convective heat transfer in the enclosure is based on two-dimensional, incompressible, laminar flow in Cartesian coordinate system. The equations are well known:

$$\frac{\partial U}{\partial x}+\frac{\partial V}{\partial y}=0 \tag{1}$$

$$U\frac{\partial U}{\partial x}+V\frac{\partial V}{\partial y}=-\frac{1}{\rho}\frac{\partial p}{\partial x}+\nu\nabla^2 U \tag{2}$$

$$U\frac{\partial V}{\partial x}+V\frac{\partial V}{\partial y}=-\frac{1}{\rho}\frac{\partial p}{\partial y}+\nu\nabla^2 V+g\left[\beta_T\left(T-T_{ref}\right)\right] \tag{3}$$

$$U\frac{\partial T}{\partial x}+V\frac{\partial T}{\partial y}=\alpha\nabla^2 T \tag{4}$$

Where U and V are the velocity components in x and y directions respectively, ρ is the density of the fluid, p is the total pressure and ν is the kinematic viscosity of the fluid. The gravity acceleration is defined by g and β_T is the thermal expansion coefficient. T and T_{ref} are the temperature and the reference temperature, respectively, and α is the thermal diffusivity. The transport dimensionless parameters, the Grashoff (Gr), the Prandtl (Pr) and the Rayleigh number (Ra) are given by:

$$Gr=\frac{g\beta_T\Delta T H^3}{\nu^2},\ \mathrm{Pr}=\frac{\nu}{\alpha} \tag{5}$$

$$Ra=Gr\cdot\mathrm{Pr} \tag{6}$$

3. NUMERICAL MODEL

The solution domain is divided into a number of rectangular control volumes (CV), resulting in a structure orthogonal non-uniform mesh. Grid points are located according to a cell-centered scheme and velocities are store in a collocated arrangement [11]. A typical CV with its main dimensions and internodal distances is sketched in Fig. 1. Writing equations (1), (2), (3) and (4) in terms of a general variable $\varphi=\{1,U,V,T\}$ with $\Gamma_\varphi=\left\{0,\mu,\mu,{}^{\mu}\!/_{\mathrm{Pr}}\right\}$ and $S_\varphi=\left\{0,-\frac{\partial P}{\partial x},-\frac{\partial P}{\partial y},0\right\}$ one gets

$$\frac{\partial}{\partial x}\left(\rho U\varphi - \Gamma_\varphi \frac{\partial \varphi}{\partial x}\right) + \frac{\partial}{\partial y}\left(\rho V\varphi - \Gamma_\varphi \frac{\partial \varphi}{\partial y}\right) = S_\varphi \tag{7}$$

After integrating it over the CV of Fig. 1,

$$\int_{\delta V}\left[\frac{\partial}{\partial x}(\rho U\varphi) + \frac{\partial}{\partial y}(\rho V\varphi)\right]dV = \int_{\delta V}\left[\frac{\partial}{\partial x}\left(\Gamma_\varphi \frac{\partial \varphi}{\partial x}\right) + \frac{\partial}{\partial y}\left(\Gamma_\varphi \frac{\partial \varphi}{\partial y}\right)\right]dV + \int_{\delta V} S_\varphi dV \tag{8}$$

Integration of the three terms in (8), namely: convection, diffusion and source, lead to a set of algebraic equations. These practices are described elsewhere [e.g see details in reference Patankar (1980)] and for this reason they are not repeated here. In summary, convective terms is discretized using the upwind differencing scheme (UDS), diffusive fluxes make use of the central differencing scheme.

Substitution of all approximate expressions for interface values and gradients into the integrated transport equation (8), gives the final discretization equation for grid node P

$$a_P\varphi_P = a_E\varphi_E + a_W\varphi_W + a_N\varphi_N + a_S\varphi_S + b \tag{9}$$

With the east face coefficient, for example, being defined as:

$$a_E = \max\left[-C_e, 0\right] + D_e \tag{10}$$

In (10), $D_e = \mu_e \delta_y / \Delta x_e$ and $C_e = (\rho U)_e \delta_y$ are the diffusive and convective fluxes at the CV east face, respectively, and, as usual, the operator $\max[a,b]$ returns the greater between a and b.

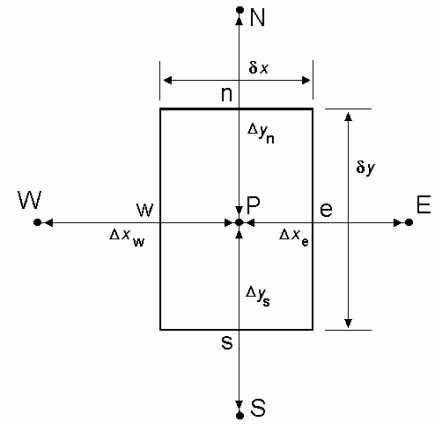

Fig. 1– Control Volume for discretization.

4. MULTIGRID TECHNIQUE

The present development about the Multigrid technique it also was presented in[Rabi and De Lemos (2001), Rabi and De Lemos (2003), Mesquita and De Lemos (2005), Mesquita and De Lemos (2007)] for this reason the development is not repeated here. If an iterative scheme as the one described below is applied to the system of equations on a given grid, it turns out only those frequencies of the solution error can be reduced efficiently, which corresponds to the grid spacing. The high frequencies of the error are reduced a few iterations, while the low frequencies nearly remain unchanged. The basic idea of a Multigrid method is to involve a hierarchy of successively coarsened grids into the iterative solution process. Following an adequate strategy for the movement through the different grid levels, and transferring data consistently with the discretization scheme between the grids, this result in an efficient error reduction over a wide spectrum of frequencies. The effect of such a Multigrid approach is that the convergence rate becomes independent on the grid spacing and the numerical solution faster.

5. RESULTS AND DISCUSSION

The developed computer code was run on an IBM PC machine with a processor INTEL CORE 2 DUO 2.0 GHz. Grid independence studies were conducted such that the solutions presented herein are essentially grid independent. For both cycles, pre- and post-smoothing iterations were accomplished via the Gauss-Seidel algorithm while, at the coarsest-grid, the TDMA method has been applied [Mesquita and De Lemos (2007)]. Also, the geometries of Fig. 2 a) and were run with the finest grid having sizes of $66x66$ grid points, Fig. 2 b).

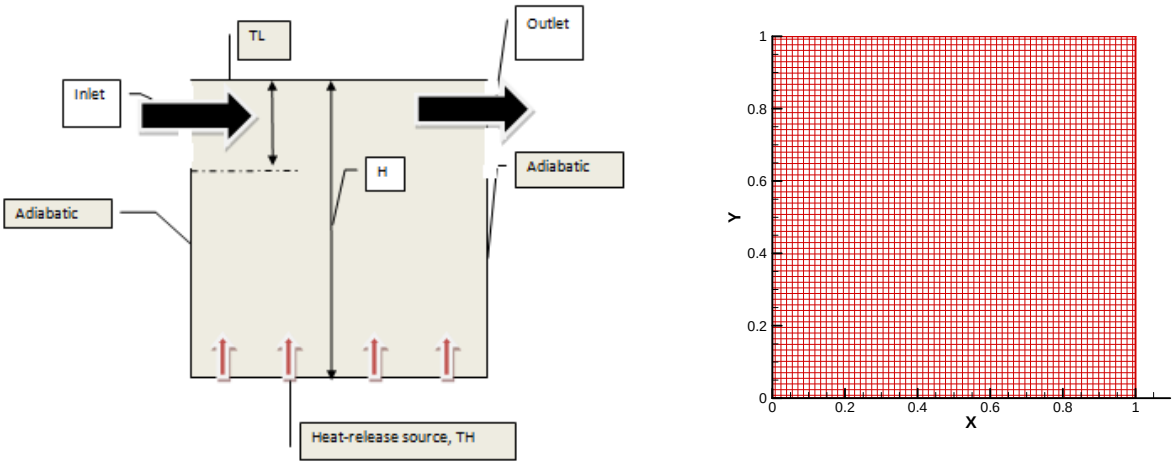

Fig. 2 - a) Geometries and boundary conditions and b) computational grid.

However, Fig. 3 shows the streamlines and isotherms, respectively, of a clear square cavity heated on the left and cooled from the opposing side for Rayleigh numbers ranging from 1×10^3 to 1×10^6. At $Ra=1\times10^3$, the streamlines in Fig. (3a) indicates the existence of a single vortex with center in the middle of the cavity.

(3b) are almost parallel to the heated walls, indicating that most of the heat transfer is transferred by conduction. The vortex is generated due the horizontal temperature gradient across the section. This gradient, $\frac{\partial T}{\partial y}$ is negative everywhere, inducing a clockwise oriented vorticity. When the Rayleigh number is increased to $Ra=1\times10^4$, Fig. (3c), the central vortex is distorted into an elliptic shape and the effect of convection is more pronounced in the isotherms, Fig. (3d). Temperature gradients are stronger near the vertical walls, but decrease in the center region. For $Ra=1\times10^5$, Fig. (3e), the behavior continues. The central vortex is elongated and two secondary vortices appear inside it. Heat transfer by convection in the viscous boundary layer alters the temperature distribution to such an extent that temperature gradients in the center of the domain are close to zero. Fig. (3e) show that, with this change in the sign of the source term negative vorticity is induced within the domain. This also causes the development of secondary vortices in the core.

Fig. 4 shows the residue history for temperature with different values of $Ra=1\times10^3$ to 5×10^5, up to 3 grids, for the V- and W-cycles. For the three grids, a slight advantage in using the W-cycle is observed in Fig.4. The exception of this rule, it is the case where the $Ra=1\times10^5$. Practically the numerical solution using the V – or W- cycle has the same performance. In this sense, for this specifically example, independent of the choosing option of the Multigrid strategies, the performances of the Multigrid algorithm were much closed. For recirculating flows, the better performance of W-cycles over the sweeping strategies is documented in the literature [Rabi and De Lemos (2001),Rabi and De Lemos (2003),Mesquita and De Lemos (2005)].

Fig. 5 shows the isotherms and streamlines of a clear square cavity heated on the bottom and cooled from the top for Rayleigh numbers with $Ra=4\times10^4$ for the present results and the results were obtained by [Braga (2003)]. As can note, the results are very close. Fig. shows the circulatory motion brings the bottom hot temperature stream up to the top wall, substantially penetrating into the flow core. Additionally the Fig. 5 represent only one of the possible solutions for that Ra number.

Fig. **6** shows for the case of the Richardson number ($Ri=2$) for different values of the Grashof number ($Gr=10^{+03}$ to $Gr=8\times10^{+04}$) is considered and also verification of the influence of $w=0.10$ in the pattern of the aiding flow. Here the buoyancy-induced flow and the forced flow aid each other in increasing the streamlines. To

examine the flow behavior more closely, the visualization of the streamlines and isothermal lines is plotted for various values of Gr, in Fig. **6**. As Gr increases there's the increase the nature flow region and the recirculation cell is characterized by one primary recirculating clockwise vortex that occupy the central region and the convective character of isothermal lines is more prominent, with another words, the convection heat transfer has become the principal energy carrier in this cases.

Fig. **7** presents the influences of size of heated area in the pattern of flow when is considered different values of width of inlet (w), firstly is considered that cavity is heated from below only in the 20 % of south wall for three different values of $w = 0.10, 0.30 \text{ and } 0.50$. The flow patterns are characterized by two recirculating clockwise vortex (different size) one localized in the middle part of cavity and another one, more closed the left wall. As the w is increased for 0.30, the two vortices is joint in only principal vortex and when the w is assumed equal to 0.50, the big one is divided again in two different vortex , as shown in the Figure. For the case that was considered the entire south wall heated the pattern of flow and thermal field are completely different , for specific condition , is easy to note that influence of convection transport are dominant.

6. CONCLUSION

The current investigation addressed two-dimensional laminar mixed convection in vented-cavity totally filled with air ($\text{Pr} = 0.71$) for suitable combinations of several different values of Reynolds number and Richardson numbers. The effects of varying both Reynolds and Richardson numbers on the resulting convection are investigated. Interesting behaviors of the flow and thermal fields with varying Reynolds and Richardson are observed, when the width of heated section is decreased or increased. For $Ri = 2$ is united with different values of w and the length of heated wall , at least two primary vortex are observed in the central position of the cavity, as the heated section is increased , the two vortex are amalgamated and only one extensive vortex persisted. In all the cases considered here, the multigrid solution represented the option with less computational effort.

7. ACKNOWLEDGEMENTS

The authors are indebted to CNPQ and CAPES, Brazil, for their invaluable support during the course of this research endeavor.

Stream functions

Temperature

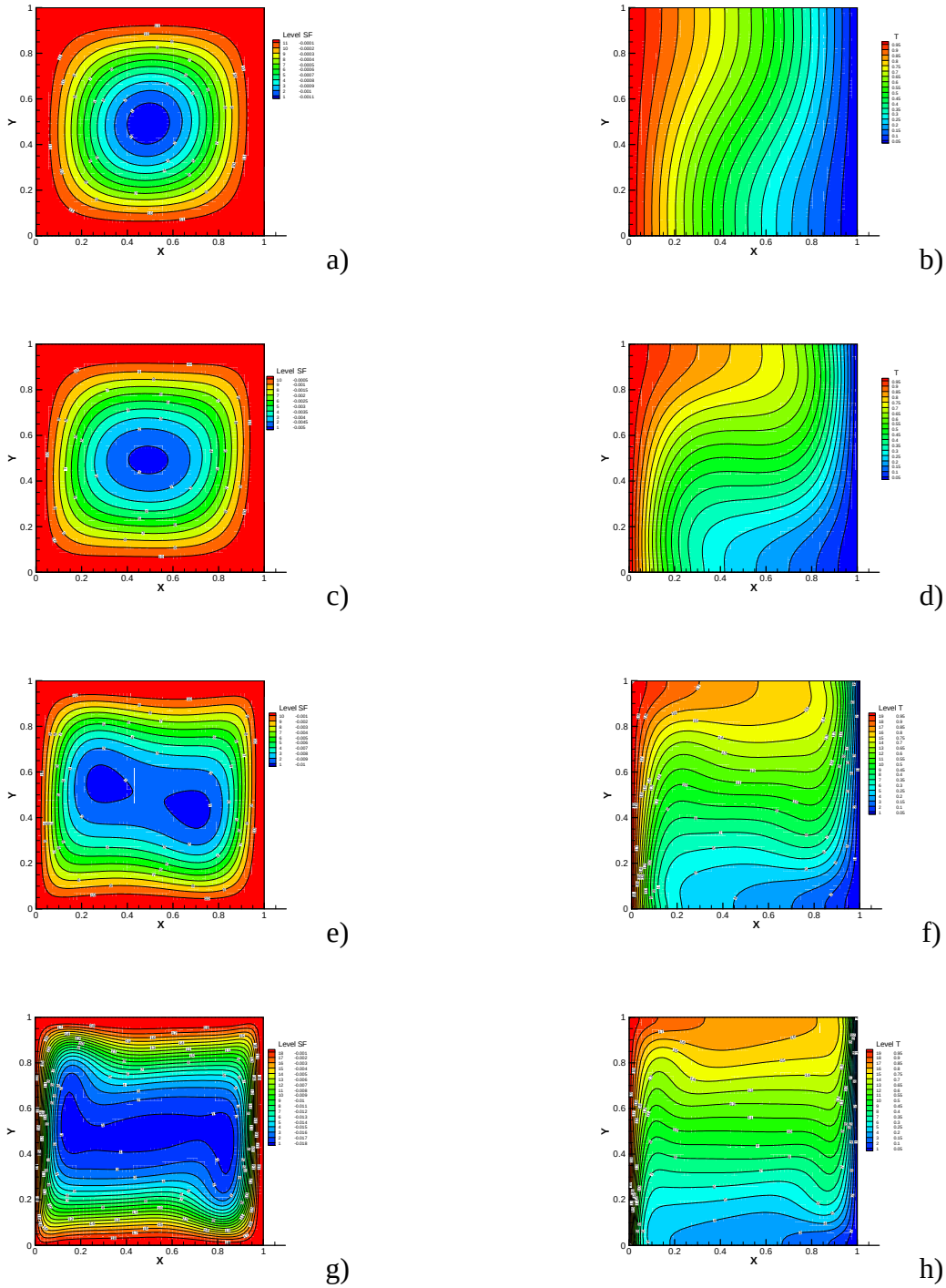

Fig. 3 - Natural Convection in Square Cavity from left to bottom $Ra = 1\times10^{3}$, $Ra = 1\times10^{4}$, $Ra = 1\times10^{5}$ **and** $Ra = 1\times10^{6}$, **respectively**

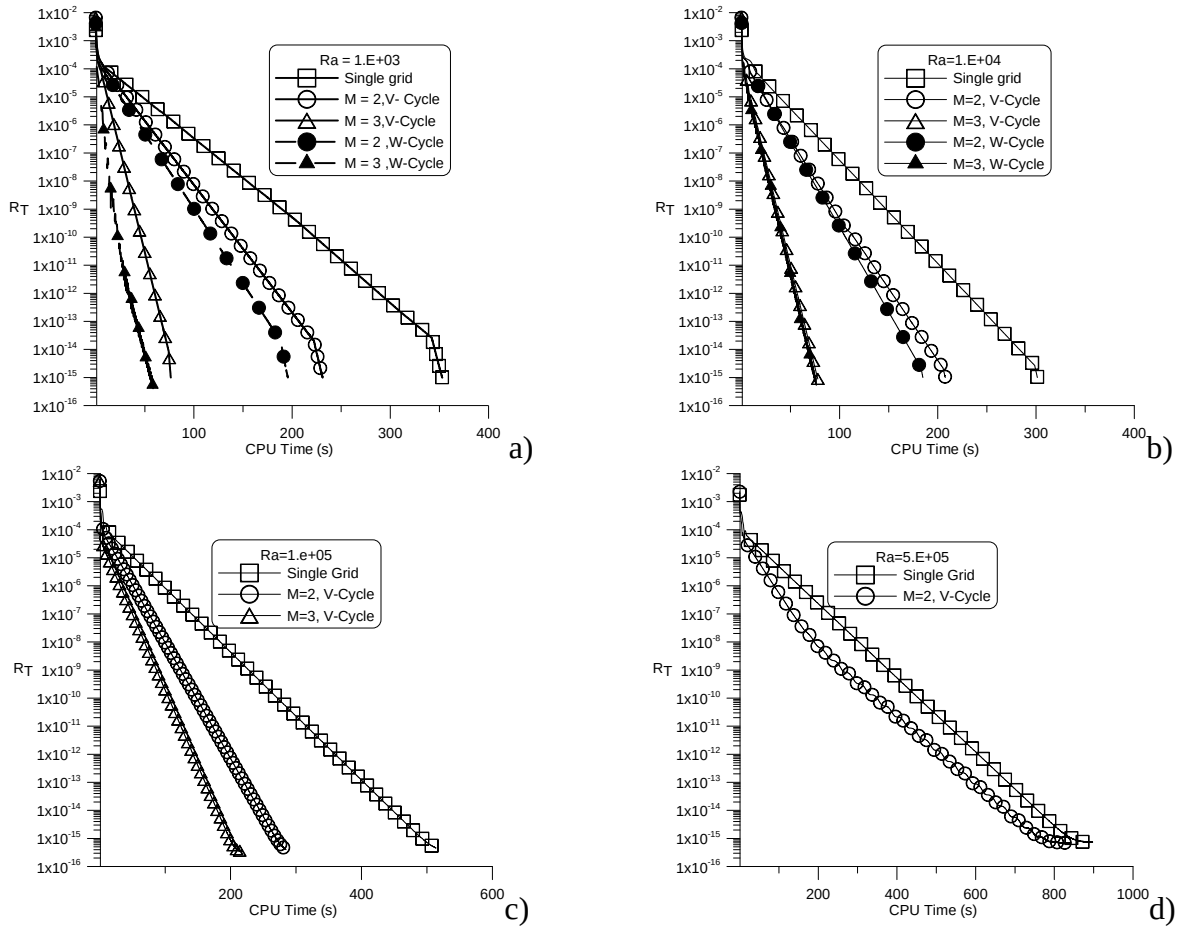

Fig. 4 – Temperatures residues history for different values of the Rayleigh number: a) $Ra = 1\times10^{3}$**, b)** $Ra = 1\times10^{4}$**, c)** $Ra = 1\times10^{5}$ **and d)** $Ra = 5\times10^{5}$

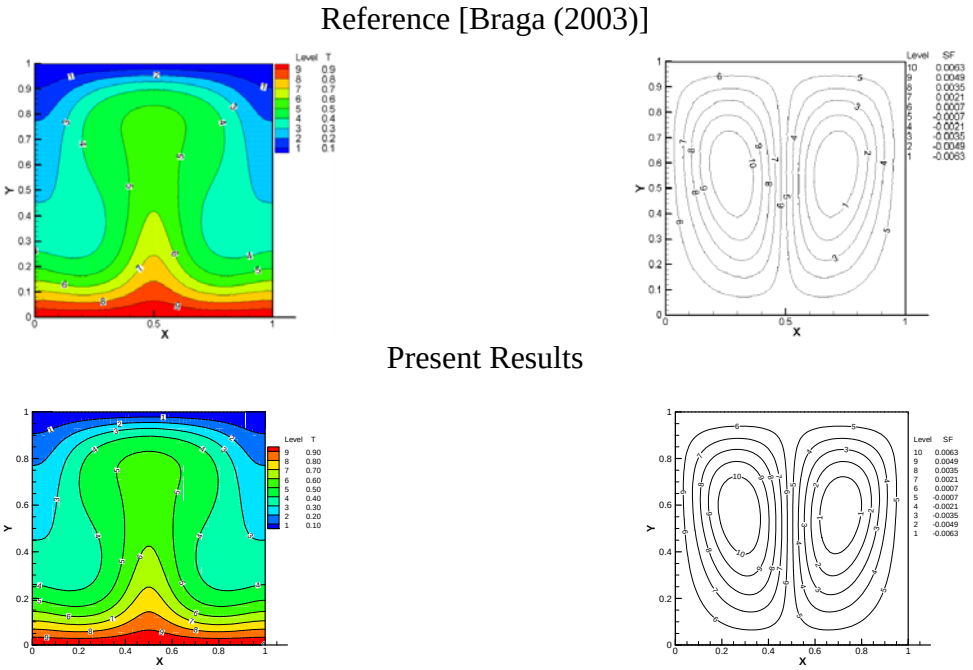

Fig. 5 – Isotherms and Streamlines for a clear square cavity heated from bottom and from the ceiling for $Ra = 4\times10^{4}$**, comparison between [1] and present research.**

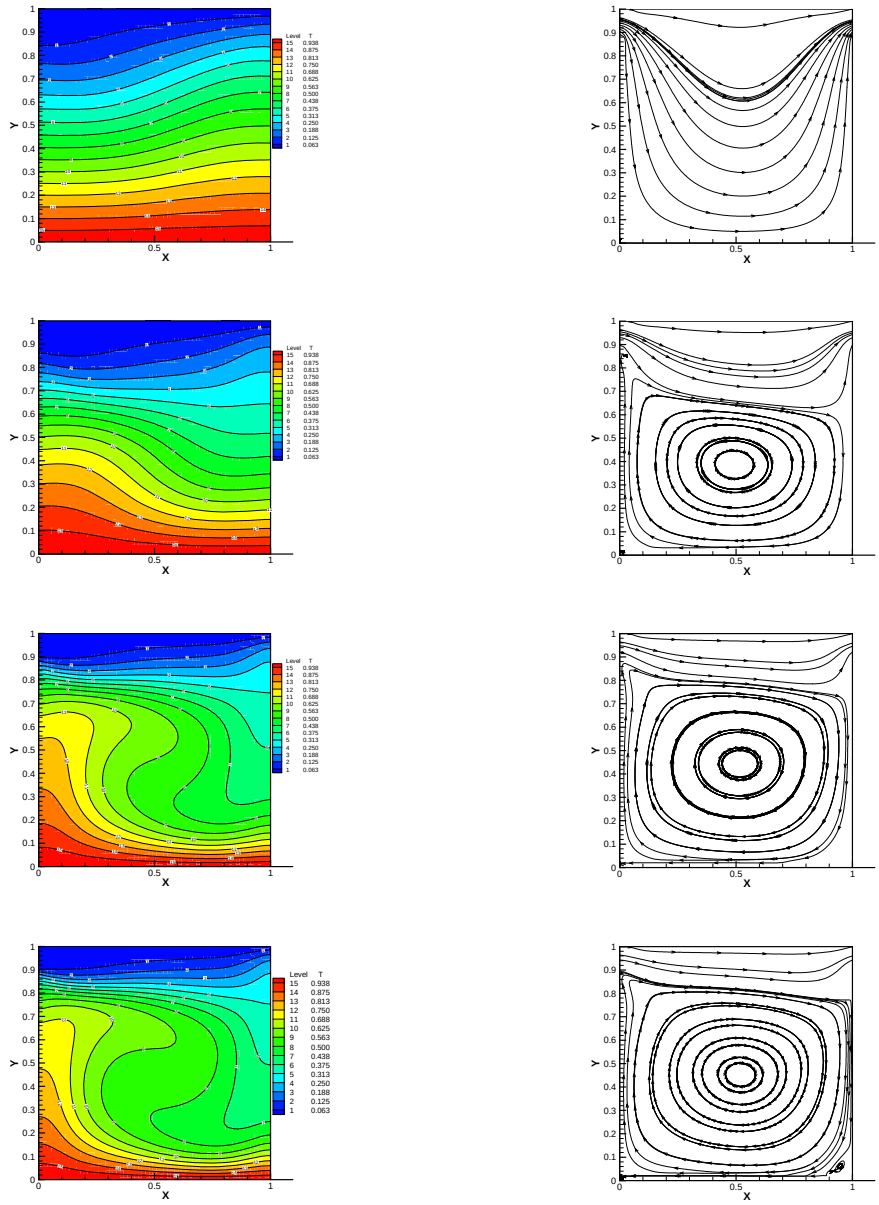

Fig. 6 – Isotherms and Streamlines for a clear mixed square cavity heated from bottom $Ri = 2$, $w = 0.10$: a) $Gr = 10^{+03}$, b) $Gr = 10^{+04}$, c) $Gr = 4 \times 10^{+04}$ and d) $Gr = 8 \times 10^{+04}$.

$w = 0.10$ $w = 0.30$ $w = 0.50$

$Gr = 1\times10^{+05}$ – 20% area heated from below

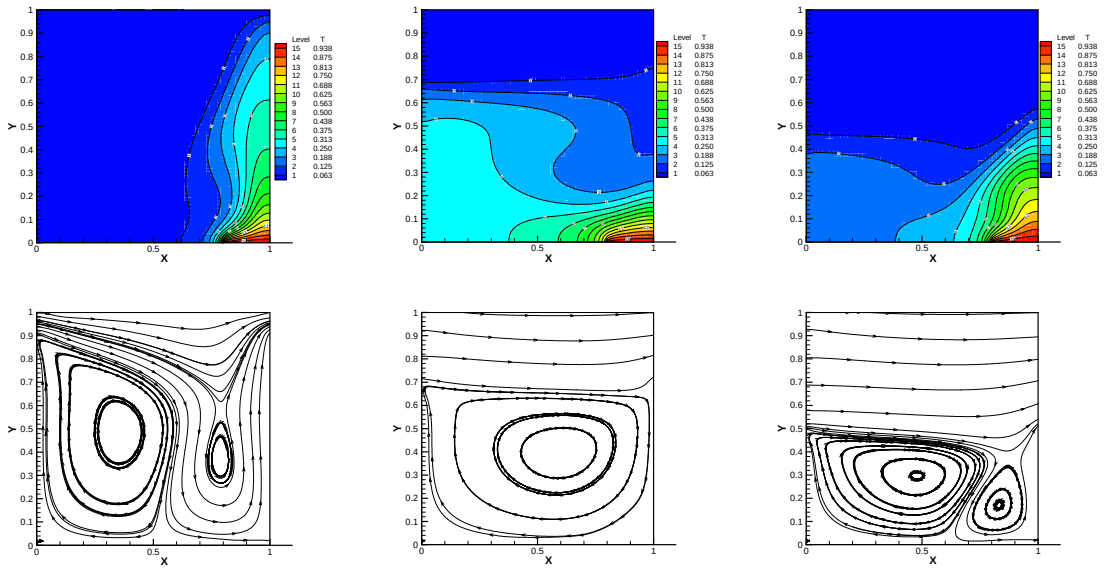

$Gr = 1\times10^{+05}$ _ Totally area heated from below

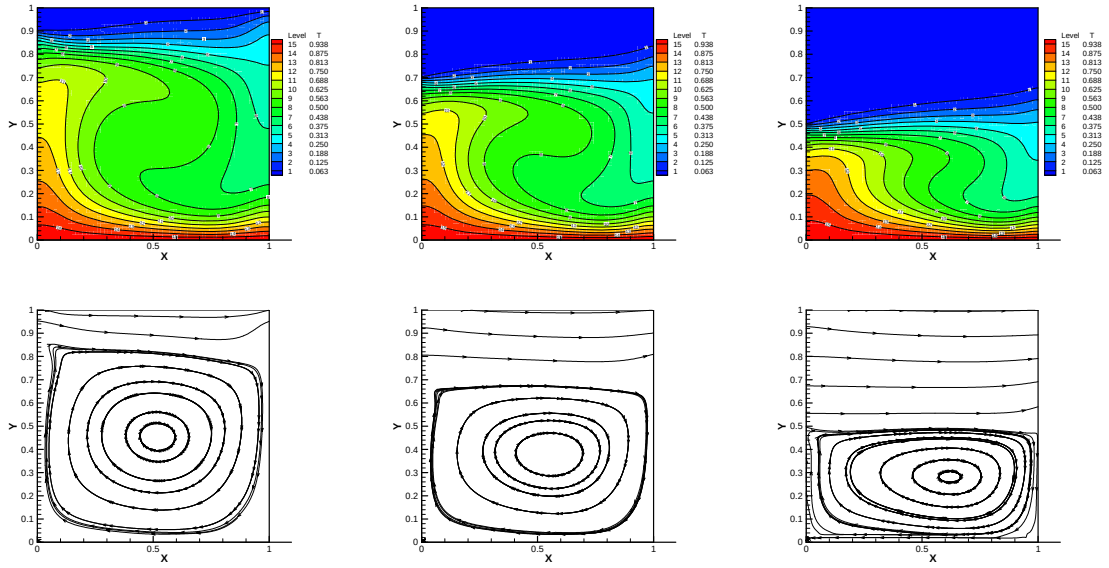

Fig. 7 – Isotherms and Streamlines for a clear mixed square cavity heated from below - influence of length of heated section.

8. REFERENCES

1. Braga, E. J., Turbulent Natural Convection in Porous Enclosures, PhD Thesis, ITA, 2003.
2. Brandt, A 1977, Multi-Level Adaptive Solutions to Boundary-Value Problems, Math. Comp., Vol. 31, No. 138, Pp. 333-390.
3. Cheikh, N. B., Brahim, B. B. , Lili, T., Influence of thermal boundary conditions on natural convection in a square enclosure partially heated from below, IJHMT, 34 (2007) 369–379.

4. De Lemos, M.J.S., Mesquita, M.S., 1999, Multigrid Numerical Solutions Of Non-Isothermal Laminar Recirculating Flows, Applications of Computational Heat Transfer, ASME-HTD-Vol. 364-3, ISSN: 0272-5673, ISBN: 0-7918-1656-7, Ed..L.C. White, Pg. 323-330.
5. Hackbusch, W., 1985, Multigrid Methods and Applications, Springer-Verlag, Berlin.
6. Jiang, Y., Chen, C.P., Tucker, P.K., 1991, Multigrid Solutions of Unsteady Navier-Stokes Equations Using a Pressure Method, Num. Heat Transfer - Part A, Vol. 20, Pp. 81-93.
7. Mesquita, M.S., de Lemos, M.J.S., 2000a, Numerical Solution of Non-Isothermal Laminar Recirculating Flows Using The Multigrid Method, ENCIT 2000, Porto Alegre, RS, Brazil, 2000.
8. Mesquita, M.S., de Lemos, M.J.S, 2004, Optimal Multigrid Solutions of Two Dimensional Convection-Conduction Problems, Applied Mathematics and Computation, v. 152, n. 3, p.725-742.
9. Mesquita, M. S.; Lemos, Marcelo Jose Santos de, 2005, Effect of Medium Properties on Convergence Rates of Multigrid Solutions of Laminar Flows in Permeable Structures. International Journal of Dynamics of Fluids Ijdf, Delhi - India, V. 1, N. 1.
10. Mesquita, M.S., de Lemos, M.J.S, 2007, Mixed Convection In Square Vented Enclosure Filled With A Porous Material Using The Multigrid Method, AIChE Annual Meeting, Conference Proceedings.
11. Patankar, S.V., 1980, Numerical Heat Transfer and Fluid Flow, Mc-Graw Hill.
12. Rabi, J.A., de Lemos, M.J.S., 2001, Optimization of Convergence Acceleration in Multigrid Numerical Solutions of Conductive-Convective Problems, Applied Mathematics and Computation, vol. 124, pp. 215-226.
13. Rabi, J.A., de Lemos, M.J.S., 2003, Multigrid Correction-Storage Formulation Applied to the Numerical Solution of Incompressible Laminar Recirculating Flows, Applied Mathematical Modeling, v.27, n.9, p.717 - 732.
14. Stüben, K., Trottenberg, U., 1982, Multigrid Methods, In Lect. Notes Math., Vol. 960, Pp. 1-76, Berlin

9. RESPONSIBILITY NOTICE

The author(s) is (are) the only responsible for the printed material included in this paper.